© 2015. Published by The Company of Biologists Ltd | Development (2015) 142, 2226 doi:10.1242/dev.126425

CORRECTION

The transmembrane protein Crumbs displays complex dynamics during follicular morphogenesis and is regulated competitively by Moesin and aPKC

Kristin M. Sherrard and Richard G. Fehon

There was an error published in *Development* **142**, 1869-1878.

On p. 1869, the sentence 'Recently, the JM domain was implicated in specifying the position of a supercellular actomyosin cable, by concentrating atypical protein kinase C (aPKC) away from the site of the cable, thereby allowing an increase in localized Rhomboid (Rho) activity (Roper, 2012).' should instead have read:

'Recently, the JM domain was implicated in specifying the position of a supercellular actomyosin cable, by concentrating atypical protein kinase C (aPKC) away from the site of the cable, thereby allowing an increase in localized Rho-kinase (Rok) activity (Roper, 2012).'

The publishers and authors apologise to readers for this mistake.

© 2015. Published by The Company of Biologists Ltd | Development (2015) 142, 1869-1878 doi:10.1242/dev.115329

RESEARCH ARTICLE

The transmembrane protein Crumbs displays complex dynamics during follicular morphogenesis and is regulated competitively by Moesin and aPKC

Kristin M. Sherrard and Richard G. Fehon*

ABSTRACT

The transmembrane protein Crumbs (Crb) functions in apical polarity and epithelial integrity. To better understand its role in epithelial morphogenesis, we examined Crb localization and dynamics in the late follicular epithelium of *Drosophila*. Crb was unexpectedly dynamic during middle-to-late stages of egg chamber development, being lost from the marginal zone (MZ) in stage 9 before abruptly returning at the end of stage 10b, then undergoing a pulse of endocytosis in stage 12. The reappearance of MZ Crb is necessary to maintain an intact adherens junction and MZ. Although Crb has been proposed to interact through its juxtamembrane domain with Moesin (Moe), a FERM domain protein that regulates the cortical actin cytoskeleton, the functional significance of this interaction is poorly understood. We found that whereas the Crb juxtamembrane domain was not required for adherens junction integrity, it was necessary for MZ localization of Moe, aPKC and F-actin. Furthermore, Moe and aPKC functioned antagonistically, suggesting that Moe limits Crb levels by reducing its interactions with the apical Par network. Additionally, *Moe* mutant cells lost Crb from the apical membrane and accumulated excess Crb at the MZ, suggesting that Moe regulates Crb distribution at the membrane. Together, these studies reveal reciprocal interactions between Crb, Moe and aPKC during cellular morphogenesis.

KEY WORDS: Crumbs, ERM proteins, Squamous morphogenesis, Par3/Bazooka, F-actin, aPKC

INTRODUCTION

Epithelia form the basis of animal tissue architecture, establishing a barrier against diffusion and providing mechanical structure by their adhesive and cytoskeletal properties. Apicobasally polarized membrane and junctional domains serve these functions and maintain their identities in the face of dynamic processes, such as cell cleavage, rearrangements, tissue bending, spreading and cell delamination. Understanding how cells manage this has major implications for both development and human health.

One key regulator of epithelial integrity is the apical transmembrane protein Crumbs (Crb). Crb regulates apicobasal polarity in *Drosophila* (Tepass, 1996) as well as in vertebrates (Bazellieres et al., 2009; Roh et al., 2003). More recently, Crb has been recognized as having a distinct role regulating the positioning and stability of adherens junctions (AJs) during such processes as the formation of the salivary gland and rhabdomere biogenesis during pupal eye development (Campbell et al., 2009; Klose et al., 2013; Letizia et al., 2011; Morais-de-Sá et al., 2010; Muschalik and Knust, 2011; Röper, 2012; Pocha and Knust, 2013; Tepass, 2012; Walther and Pichaud, 2010).

Crb contains several conserved domains: an extracellular domain that oligomerizes to stabilize Crb localization at the membrane (Muschalik and Knust, 2011; Pellikka et al., 2002; Richard et al., 2009; Thompson et al., 2013), and two highly conserved intracellular domains, a C-terminal PDZ-binding domain and a juxtamembrane (JM) domain (Klebes and Knust, 2000). The PDZ-binding domain interacts with the Par and Sdt complexes to promote apical polarity (Tepass, 2012). The function of the JM domain (also called the FERM-binding domain) is not as well understood. It is implicated in positively regulating Hippo (Hpo) signaling by binding Expanded (Ex) (Ling et al., 2010; Robinson et al., 2010), and, via binding of Yurt (Yrt), negatively regulating Crb levels at the membrane (LaPrise et al., 2006). The JM domain also promotes AJ formation (Izaddoost et al., 2002; Klebes and Knust, 2000; Pilot et al., 2006; Bulgakova and Knust, 2009), although it is unknown which proteins interact with Crb in this context. Recently, the JM domain was implicated in specifying the position of a supercellular actomyosin cable, by concentrating atypical protein kinase C (aPKC) away from the site of the cable, thereby allowing an increase in localized Rhomboid (Rho) activity (Röper, 2012).

Many, if not all, functions of the JM domain appear to be related to the cortical actin cytoskeleton. One potential mechanistic link between Crb, the cytoskeleton and AJs is Moesin (Moe), an apical FERM protein that organizes actin and cross-links apical membrane and the actin cortex (Bretscher et al., 2002; Fehon et al., 2010; Polesello et al., 2002). Moe forms a complex with Crb, actin and β-heavy spectrin (β Spectrin; Médina et al., 2002a), and has been shown to interact with Crb in tracheal morphogenesis (Kerman et al., 2008; Letizia et al., 2011). Furthermore, Crb3, a mouse Crb ortholog, has been shown to interact with ezrin (Ezr), a mammalian Moe ortholog, and *Crb3*-knockout mice display phenotypes similar to *Ezr* mutants (Whiteman et al., 2013).

The mechanisms by which the Crb JM domain promotes epithelial integrity have remained elusive (Fletcher et al., 2012; Röper, 2012). Employing a knock-in allele of *crb* with defective FERM-binding (Huang et al., 2009), and manipulating Crb and Moe expression, we examined interactions between Moesin and the Crb JM domain in *Drosophila* main-body follicle cells (FCs). These cells form a monolayer epithelium that covers the oocyte and nurse cells, and undergo a series of dramatic cell shape changes, culminating in squamous expansion as nurse cells rapidly dump their contents into the oocyte.

Manipulating Crb and Moe expression had strong effects on junctional protein localization during the columnar-squamous transition. Crb was dynamically deployed in stages 10-12, with

Department of Molecular Genetics and Cell Biology, University of Chicago, 920 E. 58th Street, Chicago, IL 60637, USA.

*Author for correspondence (rfehon@uchicago.edu)

Received 15 July 2014; Accepted 23 March 2015

Development (2015) 142, 1869-1878 doi:10.1242/dev.115329

a previously unrecognized loss and subsequent relocalization to the marginal zone (MZ) after stage 10b, at which time it became required for maintenance of both the AJs and the MZ. From stage 11 onwards, Crb was essential for Moe localization at the MZ, whereas Moe in turn regulated Crb levels apically via actin organization, and, at the MZ, through an antagonism with aPKC that reduced Crb interaction with the apical Par network.

RESULTS

Crumbs localization shifted in conjunction with squamous morphogenesis in main-body FCs

We assessed localization of apical and junctional proteins in FCs during stages 8-12. The follicular epithelium undergoes transitions among cuboidal, columnar and squamous shapes during egg chamber development (Fig. 1A). The main body FCs become columnar in stages 9-10a, then cuboidal in stage 10b. In stage 11, they rapidly become squamous, doubling their apical and basal areas and trebling their perimeters in 20 min. Whereas external forces drive this squamous expansion as nurse cells empty their contents into the oocyte, the FCs must nevertheless actively remodel their junctions and membrane domains to maintain adhesion to the extracellular matrix (Delon and Brown, 2009; Schotman et al., 2008), cell-cell adhesion (Pope and Harris, 2008) and epithelial integrity. Because optical constraints make it difficult to image squamous cells in cross-section, we employed maximal projections encompassing the apical junctions and apical surface (see Materials and Methods and supplementary material Fig. S1 for an explanation).

Crb is normally localized in the apical region, with a high concentration in the MZ. Strikingly, in stages 9 and 10, Crb relocalized from the MZ, where it was found in stage 8 and earlier, to the apical surface (Fig. 1B), coinciding with the outgrowth of follicle cell microvilli (supplementary material Fig. S2A; see also

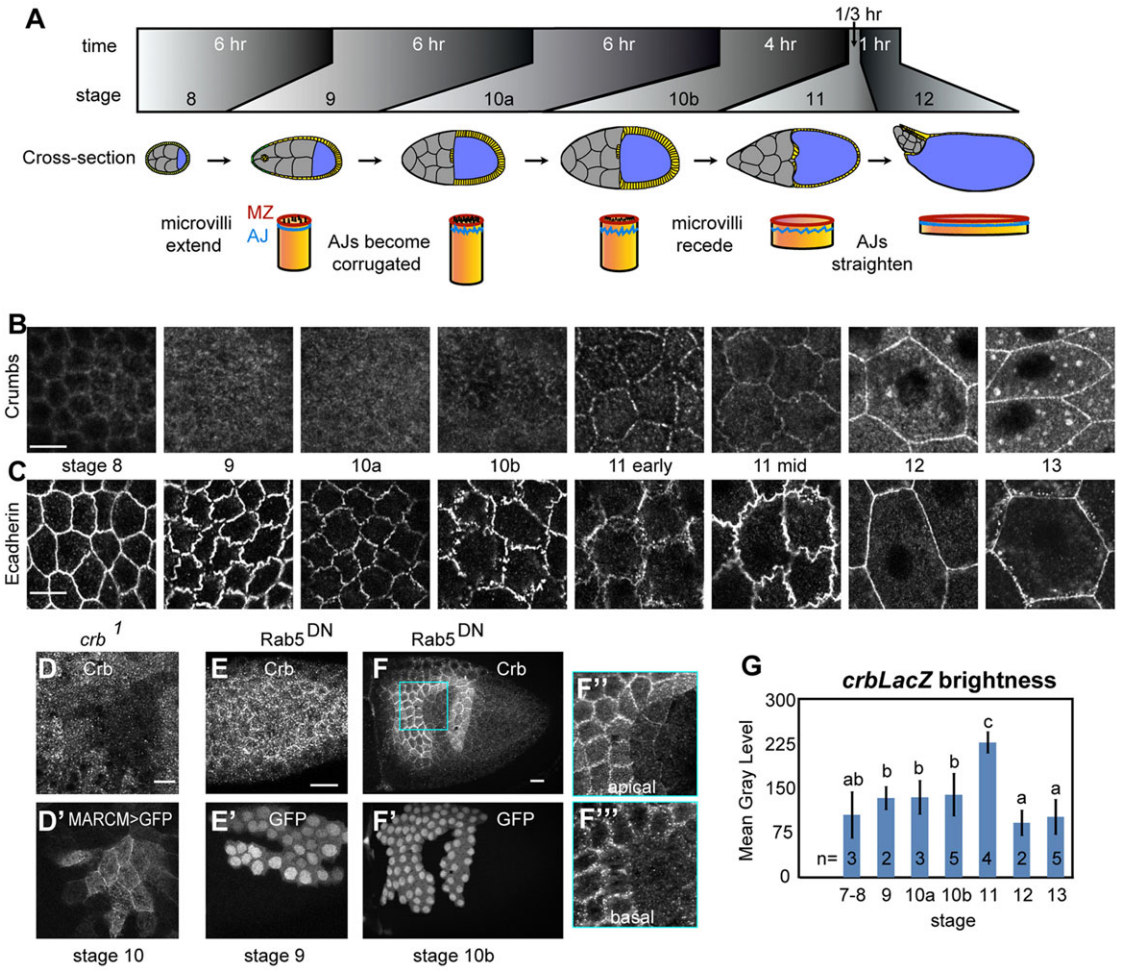

Fig. 1. Crumbs localization shifts in conjunction with squamous morphogenesis in FCs. (A) Major events during oogenesis stages 8-12: main body FCs (yellow) become columnar in stages 8-10a, then cuboidal and finally squamous, flattening in 20 min in stage 11 as the nurse cells (gray) dump their contents into the oocyte (blue). (B) Crb was lost from the MZ in stages 9-10, reappearing abruptly at the beginning of stage 11. Images are projections of four confocal sections, 0.3 µm apart, spanning the MZ and apical surface, imaged and processed with the same settings. Throughout the article, maximal projections encompassing the apical junctions and apices are shown, except where noted. (C) Ecad became highly corrugated in stages 9-11, straightening in 11-12; single sections were imaged and processed with the same settings. (D) Crb was present on follicle cell apices in stage 10, not merely on the oocyte surface, as shown by *crb*^{1} null mitotic-follicle cell clones positively labeled with MARCM. (E-F‴) Inhibiting endocytosis with flip-out clones expressing GFP and dominant-negative Rab5 (Rab5^{DN}) did not affect Crb levels in stage 9 (E,E′), in contrast to stage 10 and later, in which it caused a strong buildup of Crb (F,F′). Close-up views of Crb staining in Rab5^{DN} show apical buildup (F″) and lateral accumulation (F‴). (G) Crb transcription was upregulated in stages 9-11 relative to other stages, shown by mean gray levels of β-galactosidase in *crb lacZ* (*crb*^{M1M2}) egg chambers. Scale bars: 10 µm (in C-E), 20 µm (in F,G). Error bars in G are s.e.m., *n* shows number of egg chambers measured (10-20 cells/egg chamber). Groups labeled a-c delineate those significantly different in unpaired, two-tailed *t*-tests, to $P<0.01$.

Development (2015) 142, 1869-1878 doi:10.1242/dev.115329

D'Alterio et al., 2005; Schlichting et al., 2006). That the FCs retained apical Crb during stage 10 is confirmed by the loss of staining in *crb* null clones (Fig. 1D). Crb returned abruptly to the MZ in stage 11, just before the rapid flattening of FCs, and, in stage 12, was also present in cytoplasmic punctae.

Ecadherin (Ecad; also known as Shotgun/Shg) also changed localization during these stages. The apical-most population of Ecad (Fig. 1C) became increasingly corrugated in stages 9-10 and junctions appeared discontinuous in stage 10. In stage 11, Ecad was again continuous and straightened in conjunction with squamous expansion.

Other apical and MZ components displayed similar but less dramatic shifts in localization (supplementary material Fig. S3). Bazooka/Par3, an apical Par protein which regulates AJ assembly, was localized similarly to Ecad. Patj and aPKC remained weakly at the MZ through stage 10, and subsequently became more strongly junctionally localized. Echinoid (Ed) remained strongly junctionally localized throughout these stages. By contrast, phospho-Moe (pMoe, the active form of Moe), like Crb, lost its junctional localization in stages 9-10 but regained it by stage 12.

The rapid shifts in Crb staining could result from changes in Crb turnover from the plasma membrane via endocytosis and/or changes in *crb* transcription. Using a dominant-negative form of Rab5 ($Rab5^{DN}$) which blocks endocytosis, we found that Crb trafficking became more dynamic, beginning in late stage 10. Remarkably, whereas blocking endocytosis in stages 1-10a had no visible effect on Crb staining (Fig. 1E and data not shown). From stage 10b on it caused a strong Crb accumulation both apically and basally (Fig. 1F-F‴), indicating that Crb levels are negatively regulated by endocytosis at these stages. Similar effects were previously seen in wing disks (Lu and Bilder, 2005). Additionally, stages 12-early 13 exhibited a pulse of Crb vesicles; that these are endocytic could be shown by the abrogation of Crb-labeled vesicles in $Rab5^{DN}$ flip-out clones (supplementary material Fig. S4A). These vesicles colocalized extensively with the lysosomal marker Lamp1, indicating that they are degraded rather than recycled (supplementary material Fig. S4B). This brief and noticeable pulse of endocytosis provides a window into regulation of Crb levels. Together, these results indicate that Crb levels are dynamically regulated during crucial stages of follicular morphogenesis.

To examine *crb* transcriptional regulation in the follicular epithelium, we employed a *lacZ* reporter for *crb* expression (Herranz et al., 2006). We found that return of Crb to the MZ in stage 11 was preceded by a strong upregulation in *crb* transcription (Fig. 1G). Thus, transcriptional regulation of *crb* expression also plays a role in its dynamic expression patterns in the follicular epithelium.

Crb is required for localization of MZ and AJ proteins beginning in stage 11

Increased Crb expression flattens embryonic epidermal cells by increasing their apical domain at the expense of the lateral domain (Wodarz et al., 1995), although it has also been suggested that increased levels of endogenous Crb cause expansion of the MZ and a corresponding reduction of the apical, free surface (Letizia et al., 2013). We tested whether FCs might regulate Crb to facilitate rapid apical expansion. However, depleting Crb in flip-out clones using RNAi effectively reduced Crb levels, but did not prevent the apical expansion of FCs (Fig. 2A′).

Next, we considered whether the reappearance of Crb at the MZ might restructure the apical junctions. We therefore compared effects of Crb depletion at stage 10, when Crb is

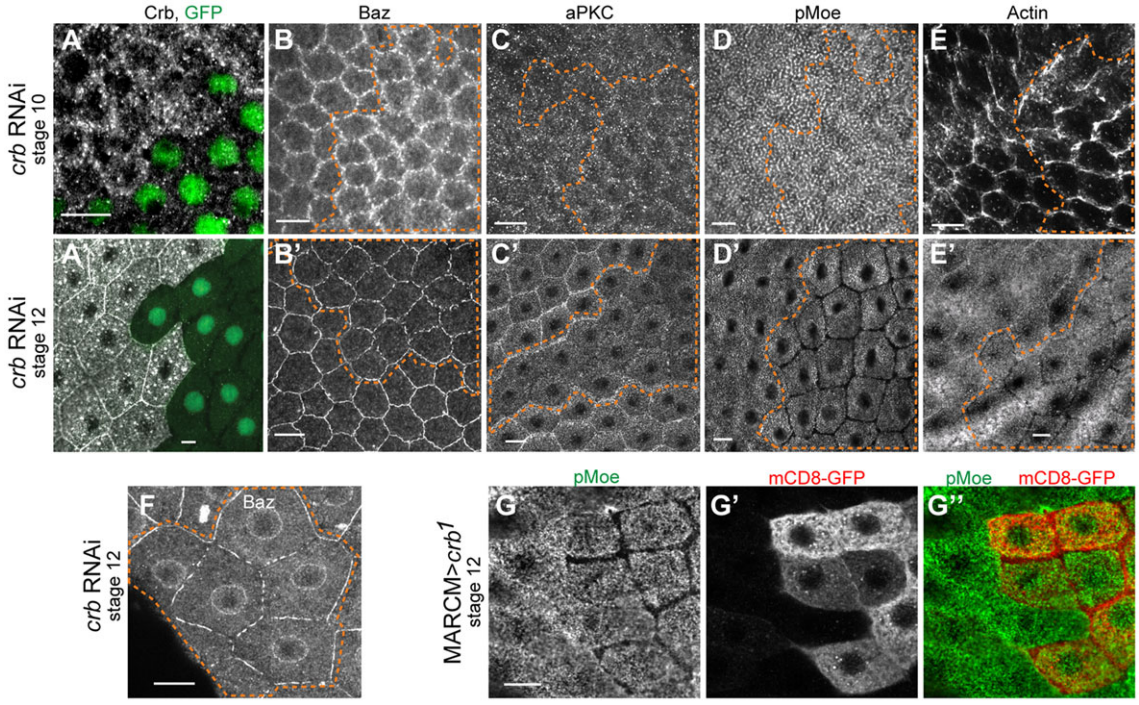

Fig. 2. Crumbs is required to localize MZ and AJ components only after stage 10. (A) Driving *crb* RNAi in flip-out clones, positively labeled with GFP, caused strong loss of Crb, which, however, did not prevent cell expansion in stage 12 (A′). (B,C,D,E) *crb* depletion did not affect AJ or MZ proteins in stage 10, when Crb is normally absent from the MZ. However, *crb* RNAi caused gaps in Baz and loss at the MZ by stage 12 (B′,C′,D′,E′). (F) High-magnification view of Baz staining in *crb* RNAi cells. (G-G″) Single-section staining of pMoe and mCD8-RFP in crb^{1} null clones show that absence of pMoe staining does not correspond to a gap between cells. Dashed lines show *crb RNAi* flip-out clones (on the right hand in all images); in all figures, the outlines are placed slightly outside the clone MZ to show border with wild-type cells. Scale bars: 10 µm.

Development (2015) 142, 1869-1878 doi:10.1242/dev.115329

not normally present at the MZ, with those at stages 11-12, when it is. If return of Crb to the MZ promotes proper organization of the MZ and AJs, then loss of Crb should affect those junctions only after stage 11. Indeed, in stage 10, Crb loss had no effect on localization of Baz, aPKC, F-actin or pMoe (Fig. 2B-E). By contrast, beginning in stage 11, Crb loss was associated with fragmentation of Baz at the AJs (Fig. 2B′,F), and with reduction of aPKC, pMoe, and F-actin at the MZ (Fig. 2C′-E′). The pMoe phenotype was particularly striking, being completely lost from the MZ, yet retained normally in the apical domain (Fig. 2D′). Co-staining pMoe with the membrane marker mCD8RFP in *crb*^{1} (null) MARCM clones (Fig. 2G-G″) reiterated that junctional integrity remained intact in Crb-deficient cells.

In sum, many MZ and AJ components depended on the return of Crb to the MZ in stage 11. As Crb has previously been implicated in the organization of AJs through its JM domain (Izaddoost et al., 2002) and/or via interaction with Moe (Médina et al., 2002b), we next turned to dissecting the roles of the Crb JM and PDZ-binding domains in this system, testing whether the Crb-dependent loss of Moe was upstream of AJ fragmentation.

The Crb JM domain is required to localize MZ but not AJ components

We employed knock-in alleles of *crb* that replace the endogenous *crb* locus with versions containing either a deleted PDZ-binding domain (*crb*^{PDM}) or a mutated JM domain (*crb*^{JMM}) (Huang et al., 2009; and see Fig. 3A). We assessed Crb localization in mitotic clones by creating homozygous cells expressing only the mutant *crb* allele. We stained with an antibody against the extracellular domain that could detect both wild-type (wt) and mutant Crb. Unsurprisingly, given the essential role of the Crb PDZ-binding domain binding to the apical Par and Sdt complexes (Bulgakova and Knust, 2009), Crb^{PDM} was not retained at the membrane and was heavily vesicular in all stages (Fig. 3B; supplementary material Fig. S4C). However, Crb^{JMM} (Fig. 3C) displayed partial to near-normal junctional localization, with no excess Crb vesicles. In contrast to boundaries with *crb* RNAi (see Fig. 2A) or Crb^{PDM} cells, wild-type cells adjacent to Crb^{JMM} cells displayed normal MZ Crb localization, suggesting that intercellular Crb interactions could stabilize Crb^{JMM}.

The junctional retention of Crb^{JMM} let us ask whether loss of the JM domain alone caused the same reduction in junctional proteins

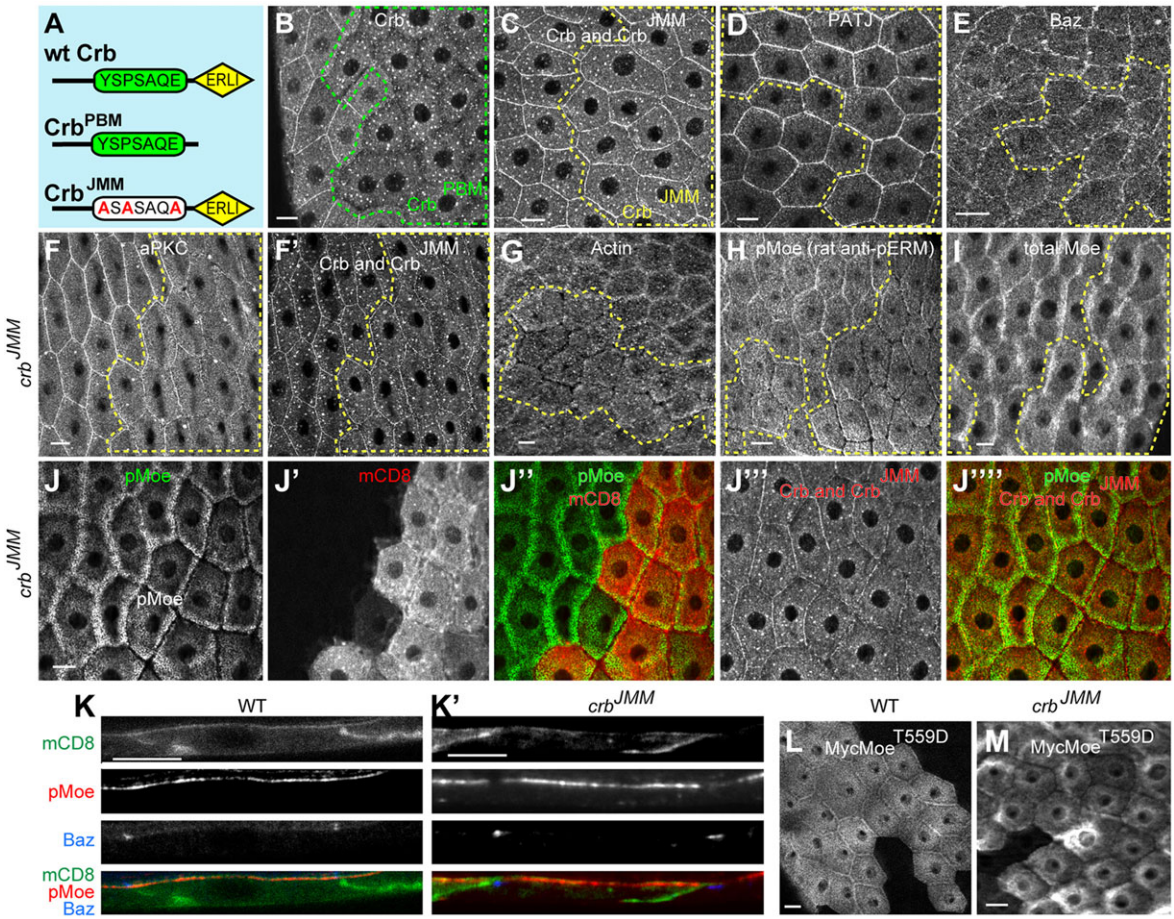

Fig. 3. Crumbs JM domain is necessary for localization of MZ proteins but not AJs. (A) Diagram of knock-in alleles deleting each of the two conserved cytoplasmic domains of Crb; extracellular domains were intact in both alleles. (B) *crb*^{PBM}, lacking the ERLI domain that binds to the apical Par proteins and Patj-Sdt complex, was unable to localize stably to the membrane and is present primarily in vesicles. (C) By contrast, the *crb*^{JMM} allele could localize to the MZ and was endocytosed at the same level as in wt cells. In *crb*^{JMM} clones, Patj (D) was normally localized, and Baz (E) was only slightly affected. However, MZ aPKC (F), F-actin (G) and pMoe (H, stained using a different fix and antibody from that in J and in Fig. 2D′,F; see Materials and Methods) were highly reduced in *crb*^{JMM} clones, although total Moe level was normal (I). (J-J⁗′) Single-section co-staining of pMoe, mCD8-GFP and Crb show that membrane is present within the gap in pMoe staining. (K,K′) Cross-sections of wild-type cells and *crb*^{JMM} clones co-stained for pMoe, Baz and mCD8. (L,M) Expressing the constitutively phosphomimetic Myc-Moe^{T559D} in *crb*^{JMM} clones showed that, relative to wild-type controls, the *crb*^{JMM} clones were still unable to localize Moe^{T559D} to the MZ. Dashed lines show *crb* knock-in allele clones (on the right hand in all images). Scale bars: 10 µm. All images show stage 12-early 13 egg chambers.

Development (2015) 142, 1869-1878 doi:10.1242/dev.115329

seen with depletion of Crb after stage 11 (except F-actin, in which neither post-fix for the Crb staining was compatible with a Phalloidin staining). We restricted our analysis to cases in which Crb^{JMM} was retained at near-normal levels. In crb^{JMM} clones, the Sdt complex member Patj localized normally (Fig. 3D), confirming that the MZ was intact. Unlike *crb* RNAi, crb^{JMM} mutants displayed near-normal localization of Baz (Fig. 3E). This indicates that, although Crb is required for AJ maintenance in this system, the key residues for FERM binding in the Crb JM domain (Klebes and Knust, 2000) are not. In contrast to Baz, we found that aPKC, F-actin and pMoe were all strongly reduced at the MZ in crb^{JMM} clones (Fig. 3F-H,J,F′ and J‴ show co-staining with Crb), much as they were with *crb* RNAi, indicating that that their normal localization requires this domain. Total Moe, however, was not affected (Fig. 3I). Note that despite the complete absence of pMoe staining, there is no physical gap between cells, as shown by MZ single-sections and cross-sections co-labeled for pMoe, mCD8 and Crb (Fig. 3K).

The Crb JM domain could either promote pMoe accumulation at the MZ or promote Moe phosphorylation specifically in that region, as suggested by the fact that total Moe localization was unaffected. To explore these possibilities more rigorously, we expressed a phosphomimetic form of Moe, Moe^{T559D}, in cells that simultaneously expressed Crb^{JMM}. We found that, although Moe^{T559D} localized properly to the MZ in wt cells (Fig. 3L), it failed to do so in Crb^{JMM}-expressing cells (Fig. 3M). Thus, the Crb JM domain is necessary to recruit active, phosphorylated Moe to the MZ in post-stage 10 FCs, but is not required for Moe phosphorylation.

A previous study (Médina et al., 2002a) showed that Crb and Moe co-immunoprecipitated from embryonic cell lysates, suggesting that they form a complex in epithelial cells. This possibility seems consistent with our observation that pMoe localization to the MZ is Crb dependent. To further examine putative binding interactions between Crb and Moe, as well as with aPKC, we performed co-immunoprecipitation experiments in S2 cells, but were unable to find any evidence for binding interactions between these proteins (supplementary material Table S1). We cannot rule out the possibility that interactions between Crb and Moe only occur in epithelial cells, but these negative results suggest that any interactions are of low affinity and possibly very transient. Nevertheless, our *in vivo* data strongly suggest that they functionally interact.

Depleting Moe causes Crb to accumulate junctionally after stage 10

If Moe functionally interacts with Crb at the MZ, then depleting Moe might affect Crb localization. Interestingly, depleting Moe had no effect on Crb in stage-10 FCs (Fig. 4A), but caused elevated MZ staining, beginning in stage 11 (Fig. 4B). We also observed a strong increase in Crb intracellular punctae at stage 12 in Moe-deficient cells (Fig. 4C), and a reduction of apical (non-MZ) Crb (Fig. 4D-F). Although Moe-depleted cells were

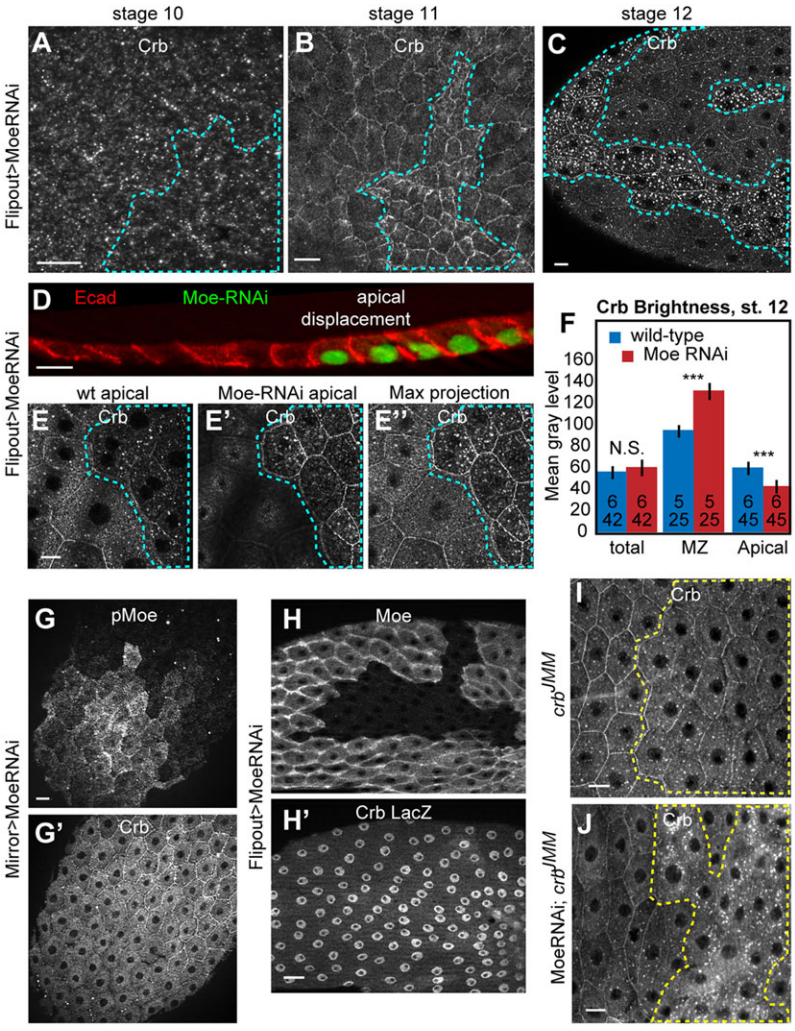

Fig. 4. In Moe-depleted cells after stage 10, Crb was excessively endocytosed, and accumulated at the MZ. Moe depletion did not affect Crb localization through stage 10 (A), but, beginning in stage 11 (B), caused accumulation of Crb at the MZ. (C) At the time wt cells endocytose Crb, Moe-depleted cells had larger and brighter Crb-stained vesicles. (D) Cross-section of stage 10 shows that *Moe* RNAi cells extend further apically than wt cells. In consequence, Moe-depleted cells are offset from wt cells, as sections E and E′ (1.2 µm apart) show; maximal projection in E″. Confocal projections shown elsewhere span the MZ to apical of wt and Moe-depleted cells. (F) Although Moe depletion did not change total Crb levels, it was associated with significantly more MZ Crb and less apical Crb. (G,G′) Depleting Moe with the weaker driver MirrorGal4, $Gal80^{ts}$ elevated MZ Crb without decreasing cell perimeter. (H,H′) Loss of Moe did not affect expression of the *crb-lacZ* transcriptional reporter. (I,J) In comparison to the crb^{JMM} mutant alone (I), depleting Moe in a crb^{JMM} mutant background reduced accumulation of Crb in the MZ. All egg chambers are stage 12, except where noted. Dashed lines show *Moe* RNAi flip-out clones or *Moe* null clones. Scale bars: 10 µm. Error bars show s.e.m.; *** denotes significant difference of $P<0.001$ by paired (values measured within the same egg chamber), two-tailed *t*-tests.

Development (2015) 142, 1869-1878 doi:10.1242/dev.115329

taller than wild-type cells, so that cell apices were offset (Fig. 4D), analysis of single sections (as shown in Fig. 4D,D′) demonstrated that Crb is lost from the apical membrane and accumulates junctionally in Moe-deficient cells (Fig. 4E). Maximal projections highlighted these changes in Crb localization (Fig. 4C,E″). To ensure that the excess MZ Crb was not due to the smaller apices of Moe-depleted cells, concentrating Crb in a smaller periphery, we confirmed that a weaker driver for the *Moe* RNAi transgene caused elevated levels of MZ Crb staining in the absence of apical shrinkage (Fig. 4G).

Because Moe is implicated in microvillar structures (Karagiosis and Ready, 2004), which, if absent during stage 10, could give rise to later phenotypes, we evaluated microvilli in *Moe* null clones and in crb^{JMM} clones. In *Moe* null clones, however, microvilli were not absent but longer than normal. Microvilli were unaffected in crb^{JMM} clones (supplementary material Fig. S2B-C″).

In agreement with the lack of change in total Crb levels (Fig. 4F), Moe depletion did not affect *crb* transcription, as measured by *crb-lacZ* expression (Fig. 4H). Furthermore, the excess Crb staining was not attributable to a complete blockage in endocytic trafficking, as Crb colocalized extensively with lysosomes in *Moe* null as well as wt cells (supplementary material Fig. S4D). Although Moe downregulates Rho1 in imaginal disks (Speck et al., 2003; Neisch et al., 2010), the Crb phenotype was independent of *Rho1* dosage (supplementary material Fig. S4E-F′).

Overall, under Moe depletion we observed a redistribution of Crb from the apical membrane to the MZ and to intracellular vesicles. This suggests that Moe functions to remove Crb from the MZ, stabilize it at the apical surface, or both, and that this is mediated by interaction with the Crb JM domain. It is also possible that some of the effects on Crb reflect a more general defect in the organization of the apical cortex and plasma membrane caused by Moe loss (supplementary material Fig. S5). To examine this possibility, we used the MARCM technique to test the effect of Moe loss on Crb^{JMM}, which should not interact directly with Moe. We observed that loss of Moe affected Crb^{JMM} localization distinctly from its effects on wild-type Crb (Crb^{+}). Whereas Moe depletion caused a buildup of Crb^{+} at the MZ, it caused a loss of Crb^{JMM} at the MZ (Fig. 4I,J). This finding suggests that Moe interaction with the JM domain might compete with another junctionally localized protein, a possibility we address below. Additionally, it suggests that Moe depletion affects Crb localization independently of the JM domain, possibly via more general effects on the actin cortex (supplementary material Fig. S5). Additionally, depletion of Moe and disruption of the actin cytoskeleton with latrunculin A similarly elevated staining for several endocytic markers in stage-12 FCs (data not shown).

aPKC stabilizes Crb at the MZ in competition with Moe

Given that the Crb JM domain was required for recruitment of both pMoe and aPKC to the MZ after stage 10 (Fig. 3F,H), we next examined potential interactions between aPKC, Moe and Crb in this system. Varying the expression of Moe or aPKC demonstrated that, beginning in stage 11 when their MZ localization became sensitive to the presence of Crb, each antagonized the localization of the other. Moe depletion caused a strong excess of both aPKC and Crb (Fig. 5A,A′), whereas overexpressing $Moe^{\Delta act}$ (a deletion that lacks the auto-inhibitory actin-binding domain and is constitutively in an open conformation; see Bretscher et al., 2002) reduced aPKC without affecting Crb (Fig. 5B,B′). Depleting aPKC in flip-out clones (driven by Act5c-Gal4) caused cell lethality by stage 9, but a milder depletion with MirrorGal4; $Gal80^{ts}$ increased MZ pMoe, even as it reduced Crb (Fig. 5C,C′). Finally, expressing constitutively active $aPKC^{CAAX}$ reduced MZ pMoe without affecting Crb (Fig. 5D,D′). Taken together with our observation that both Moe and aPKC localization at the MZ are affected by the JM mutation, these results suggest that Moe and aPKC compete for binding to the Crb JM domain.

To further test the idea that Moe and aPKC function antagonistically, we simultaneously depleted Moe and aPKC, using weakly driven RNAi that partially depleted each protein. Compared with Moe or aPKC depletion alone (Fig. 5E,F), depleting both Moe and aPKC (Fig. 5G) produced Crb junctional staining that resembled wild type (Fig. 5H, quantified in I). Although additive effects of these manipulations cannot be ruled out, the increased MZ accumulation in the double-knockdown cells is consistent with the notion that Moe and aPKC function antagonistically to regulate Crb localization at the MZ in the late follicular epithelium (Fig. 6).

DISCUSSION

Our results reveal novel functional interactions between Crumbs, Moesin and aPKC in the follicular epithelium during late stages of *Drosophila* oogenesis. We found that loss of Crb, or mutation of its JM domain, results in reduction of both aPKC and active Moe at the MZ. Surprisingly, we also found that whereas aPKC promotes MZ accumulation of Crb, Moe does the opposite – loss of Moe results in increased MZ accumulation of Crb in the follicular epithelium. These opposing phenotypes suggest that Moe and aPKC function antagonistically to regulate accumulation of Crb in the MZ at these stages.

How do Moe and aPKC regulate levels of Crb in the MZ? First, although aPKC is generally thought to interact with the Crb complex through binding to Patj and Par-6 via its C-terminal PDZ binding motif (Kempkens et al., 2006; Bulgakova and Knust, 2009; Tepass, 2012), Röper (2012) recently suggested that aPKC also interacts with the Crb JM domain. Therefore, aPKC might promote junctional localization of Crb through interaction with two Crb domains, consistent with our observation that MZ localization of Crb is partially lost in crb^{JMM} cells. In contrast to loss of aPKC, we observed excessive accumulation of Crb^{+} (and aPKC), but not Crb^{JMM}, in the absence of Moe. A previous study has proposed that Moe also interacts with the JM domain (Médina et al., 2002a), suggesting that Moe and aPKC could compete for Crb binding. Overall, we hypothesize that aPKC promotes Crb stability through interactions with the Crb JM domain, whereas Moe reduces these stabilizing interactions at the MZ through competition with aPKC (Fig. 6).

A second possible contributing factor in MZ accumulation of Crb is competition between the apical and junctional pools of Crb, with Moe functioning to stabilize apical Crb. We observed that whereas loss of aPKC does not appear to affect Crb localization at the apical membrane, reduction in Moe function caused decreased Crb on the apical membrane and increased junctional Crb. Moe might stabilize Crb at the apical membrane by linking Crb to cortical actin (Médina et al., 2002a) or through more general effects on the actin cytoskeleton. Destabilized Crb on the apical membrane could then move within the plasma membrane and/or be recycled to the MZ, where it is stabilized by interactions through its PDZ-binding domain.

Our results suggest that, in addition to the previously proposed interactions between Moe and the Crb JM domain, the more general effects of Moe on cortical actin also affect Crb localization and dynamics. In support of this idea, loss of Moe affected the localization of Crb^{JMM}, which should not be able to interact directly with Moe, and we observed pleiotropic effects on F-actin staining in

Development (2015) 142, 1869-1878 doi:10.1242/dev.115329

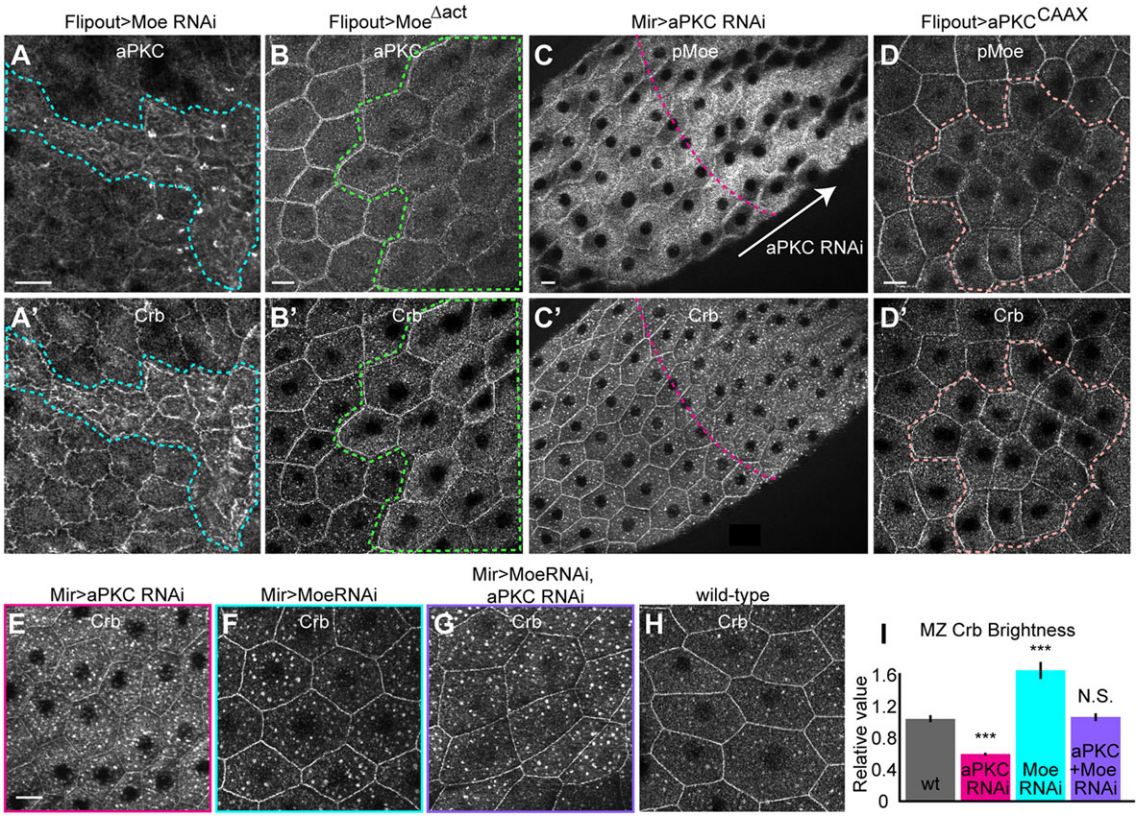

Fig. 5. aPKC stabilized Crb at the MZ in competition with Moe. Moe depletion caused buildup of both aPKC (A) and Crb (A′). Conversely, expressing Moe$^{\Delta act}$ reduced levels of aPKC (B), even while increasing Crb (B′). Partially depleting aPKC with MirrorGal4, Gal80^{ts} increased pMoe levels (C), even while decreasing Crb and increasing the number of Crb vesicles (C′). Overexpressing aPKC^{CAAX} reduced pMoe (D), while not affecting Crb levels (D′). (E) Partially depleting aPKC by RNAi using MirrorGal4, Gal80^{ts} caused loss of Crb from the MZ, as well as excessive endocytosis, relative to wt cells (H). (F) Partial depletion of Moe by RNAi with the same driver caused excessive endocytosis and excess retention of Crb at the MZ. (G) Partial depletion of both aPKC and Moe suppressed the aPKC depletion phenotype of excessive loss of Crb from the MZ and did not additively increase endocytosis, suggesting that, with reduced Moe, the remaining aPKC can secure Crb at the MZ. (I) Quantification of MZ Crb levels in G-I. Dashed lines show flip-out clones, except in C, where they show approximate boundary of MirrorGal4 driver. Scale bars: 10 µm; all images show stage-12 egg chambers.

late follicular cells depleted for Moe protein. Studies in yeast have demonstrated a crucial role for cortical actin in regulating early endocytic events (Kaksonen et al., 2006). Actin dynamics are necessary for apical endocytosis in mammalian cells (Gottlieb et al., 1993). Furthermore, the mammalian ERM protein Ezrin provides a necessary linkage to actin in the recycling of a β-adrenergic receptor (Cao et al., 1999). Further disentangling the details of the interactions between Crb, Moe and F-actin will require more specific reagents to identify and manipulate the Crb/Moe binding sites to disrupt specific functions.

Strikingly, interactions among Crb, pMoe and aPKC were evident after stage 10, coincident with an increase in Crb trafficking and MZ accumulation. Cells undergoing shape changes, such as rapid squamous expansion, must remodel their junctions and membrane domains (Goldenberg and Harris, 2013; Lecuit and Pilot, 2003; Schotman et al., 2008). Similar to the expansion of amnioserosal cells (Goldenberg and Harris, 2013; Pope and Harris, 2008), but unlike the follicle stretch cells of stage 9 (Grammont, 2007), the main-body FCs maintained continuous AJs throughout their expansion. After stage 10, MZ localization of aPKC, F-actin and pMoe, and continuity of Baz, an AJ component, required Crb. This latter result is consistent with a previous study, in which Crb was required for the addition of AJ material to the expanding rhabdomere of the pupal eye (Pellikka et al., 2002). However, another rhabodmere study using transgenic overexpression (Izaddoost et al., 2002) implicated the Crb JM domain in AJ continuity, in contrast to our finding that AJs were intact with the *crb*^{JMM} allele.

An intriguing possibility is that the putative competition between aPKC and Moe contributes to the role of Crb in morphogenesis, the mechanisms of which are not fully known (Bulgakova and Knust, 2009). In salivary placode invagination, the Crb JM domain recruits Moe and actin to a supercellular, contractile purse string (Letizia et al., 2011), which is specified by the anisotropic distribution of Crb and aPKC away from the site of the purse string (Röper, 2012). Additional evidence that the JM domain can regulate actin cable formation comes from the defective dorsal closure of *crb*^{JM} mutants (Klose et al., 2013). Our results suggest a mechanism whereby competition between Moe and aPKC for Crb JM binding could help specify an actin cable. The apical Crb-Par complex might favor aPKC binding in regions of high Crb density, but Moe binding in regions of low Crb density (such as the apical surface, or the site of the purse string in the salivary placode). Thus, competition for binding Crb could amplify the anisotropy of aPKC and Crb, and Moe could recruit the actin for the supercellular cable.

The upregulation of Crb endocytosis we observed after stage 10 probably plays a role in regulating Crb dynamics during stages 9-11. In other contexts, the retromer regulates Crb membrane levels by influencing its recycling versus degradation (Pocha et al., 2011; Zhou et al., 2011). Intercellular homophilic binding of Crb might favor its MZ localization in most tissues (Thompson et al., 2013).

Development (2015) 142, 1869-1878 doi:10.1242/dev.115329

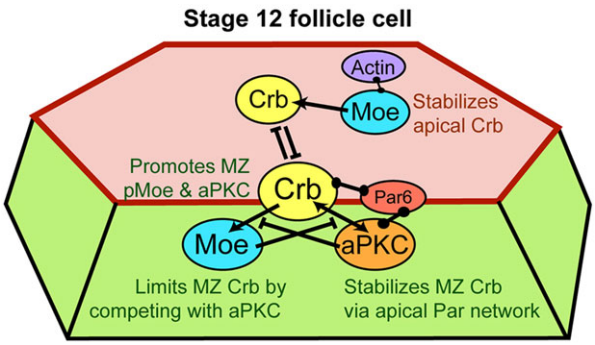

Fig. 6. Model summarizing proposed functional interaction of Crb, Moe and aPKC. Crb promotes accumulation of activated Moe at the MZ, whereas Moe, via competition with aPKC, restricts accumulation of Crb. At the apical surface, by contrast, Moe promotes Crb stability, probably via interactions with actin; thus, separate pools of apical and MZ Crb might be in competition, with apical Crb dominating in stage-10 FCs and MZ Crb in stage 11 and later. Barbell symbols indicate binding interactions, arrows indicate recruitment and barred lines indicate inhibition of localization. Red shading indicates the apical membrane, green shading indicates the lateral membrane and the red line indicates the MZ.

However, in egg chambers, the germline cells, which are tightly apposed to the apical surfaces of FCs, also express Crb (Tanentzapf et al., 2000), which could stabilize Crb apically. Thus, the outgrowth and subsequent regression of microvilli in stages 9-10 (D'Alterio et al., 2005) could drive the movement of Crb apically and back to the MZ, but this hypothesis remains untested.

A striking aspect of the effect of Crb loss on Moesin localization was that pMoe and F-actin staining appeared to be noticeably excluded from the MZ in Crb-deficient or Crb^{JMM}-expressing cells (Figs 2 and 3). In addition, the width of the zone of pMoe and F-actin loss appeared greater than the width of the MZ Crb staining. It is somewhat puzzling how pMoe and actin could be either excluded from, or fail to be recruited, to this rather broad region in the absence of the relatively narrow JM domain. One possibility is that the zone of pMoe absence represents newly added membrane material, which cannot recruit pMoe or F-actin in the absence of Crb or the Crb JM domain. Alternately, Crb might 'nucleate' addition of F-actin and/or pMoe at the MZ, and it could spread outwards from there.

The late-stage follicular epithelium displays an unexpectedly dynamic deployment of MZ components, revealing functional relationships not readily apparent in other developmental contexts. Whereas the interactions between Moe, aPKC and Crb uncover a novel connection between the apical PAR network and the apical actin cortex, much remains to be learned about how multifaceted interactions among these proteins and other junctional components direct tissue homeostasis and morphogenesis.

MATERIALS AND METHODS

Drosophila stocks and crosses

Crosses were performed at 25°C, except for $Gal80^{ts}$ crosses moved to 29°C two days before fix. Overexpression and double-stranded RNA-depletion experiments employed the UAS-Gal4 system. Flip-out expression of *act5cGal4* was driven by *hs-flippase*, heat-shocked to 37°C as pupae, 2-5 days before fix. The same method of heat shock induced mitotic recombination in clones.

Mutant strains used were Moe^{IL4} (O. Speck, PhD thesis, Duke University, 2005); crb^{M1M2} (*lacZ*) (M. Milan, ICREA, Barcelona, Spain; Herranz et al., 2006); crb^{JMM}, crb^{PBM} (Y. Hong, University of Pittsburgh, PA, USA, Robinson et al., 2010); and crb^{1} (Bloomington *Drosophila* Stock Center, Indiana University, Bloomington, IN, USA). Mutant alleles recombined with the appropriate FRT site were crossed to *hsFlp*, *Ubi-nls-RFP 19A FRT*, *hsFLP; 82B FRT Ubi-nls-RFP/TM3 Ser actGFP* or to the MARCM stocks *UAS-CD8GFP, hsFLP; tubGal4; FRT82B Gal80* (S. Horne-Badovinac, University of Chicago, IL, USA) or *FRT 19A*, *TubPGal80, hsFLP; TubPGal4, UAS-mCD8-GFP/TM3 Ser actGFP* (C. Berg, University of Washington, Seattle, WA, USA).

Transgenic lines used were $UAS\text{-}MycMoe^{\Delta act}$ (Neisch et al., 2013), $UAS\text{-}MycMoe^{T559D}$ (Speck et al., 2003), *UAS-Mer RNAi* (N. Wesolowska and R.G.F., unpublished); *UAS-Moe RNAi* (Karagiosis and Ready, 2004); *UAS-crb RNAi*, *UAS-aPKC RNAi* (Vienna *Drosophila* RNAi Center, Vienna, Austria); *ed-YFP* (Kyoto *Drosophila* Genetics Resource Center, Kyoto, Japan); *Lamp1-YFP* (Kyoto *Drosophila* Genetics Resource Center); and $UAS\text{-}Rab5^{S43N}\text{-}YFP$ (Bloomington *Drosophila* Stock Center), $UAS\text{-}aPKC^{CAAX}$ (C. Doe, University of Oregon, Eugene, OR, USA).

Immunostaining

Ovaries were dissected in Schneider's medium containing serum and fixed in 4% paraformaldehyde solution for 15 min. For Crb staining, egg chambers were post-fixed in 6 M guanadine HCl (which preserved staining of aPKC and Rabs) (Wahlström et al., 2006), or alternatively were post-fixed in methanol for 5 min. To observe pMoe localization more clearly, ovaries were fixed in 10% TCA on ice for 20 min.

Antibodies were used at the following concentrations: rabbit anti-Moe at 1:20,000 (D. Kiehart, Duke University, Durham, NC, USA), rabbit anti-phospho-ERM at 1:500 (Cell Signaling, 3141L), rat monoclonal anti-phospho-ERM at 1:20 (Matsui et al., 1998), mouse anti-Crb at 1:250 (Developmental Studies Hybridoma Bank, cq4), rat anti-DE-cadherin at 1:250 (Developmental Studies Hybridoma Bank, DCAD2), mouse anti-β-galactosidase at 1:1000 (Promega, Z3781), rabbit anti-Rab7 at 1:3000 (Tanaka and Nakamura, 2008), rabbit anti-Cadherin99c 1:1000 (D'Alterio et al., 2005), rabbit anti-Patj (M. Bhat, University of North Carolina at Chapel Hill, NC, USA), rabbit anti-aPKC at 1:500 (Santa Cruz Biotechnology, sc-216), rat anti-Bazooka at 1:250 (J. Zallen, Memorial Sloan Kettering Cancer Center, New York, NY, USA), mouse anti-Myc at 1:40,000 (Cell Signaling, 2276), guinea pig anti-hrs at 1:1000 (H. Bellen, Baylor College of Medicine, Houston, TX, USA), mouse anti-Rab11 at 1:20 (BD Transduction Laboratories, 610657), rabbit anti-GFP at 1:1000 (Molecular Probes, A-6455) and mouse anti-GFP at 1:1000 (Invitrogen, A-11120). Fluorescent secondary antibodies were obtained from Jackson ImmunoResearch Laboratories and used at a dilution of 1:1000. Oregon Green or Rhodamine Phalloidin was used at 1:200 (Invitrogen, 07466, R415) and FM4-64× at 10 µl/ml (Molecular Probes, F-34653). Tissues were mounted in ProLong Antifade (Invitrogen). Confocal images were taken on a laser-scanning confocal microscope (LSM510; Carl Zeiss), using the LSM acquisition software (Carl Zeiss) and a 40× NA 1.3 EC Plan-NeoFluar objective. Apotome images were taking using a Zeiss Axioplan 2 and a 40× NA 1.3 EC Plan-NeoFluar objective using Axiovision 4 software. Images were compiled using ImageJ (National Institutes of Health).

Quantifications of pixel intensities

Pixel intensities of *crb lacZ* and Crb were quantified as mean gray levels in ImageJ, using single slices or maximal projections of unsaturated confocal *z*-series taken at 1024×1024, 7.3 pixels/µm. For *crb lacZ* we used single slices centered on the mid-nucleus and measured an oval section excluding the nucleolus.

We defined MZ Crb staining as the two to three confocal slices (0.3 µm apart) with the brightest Crb staining at cell peripheries (supplementary material Fig. S1). Co-labeling experiments showed this region was 1-1.5 µm apical to the adherens junction staining of ECad and Baz, and coincided with aPKC and pMoe, confirming its identity as MZ. We measured Crb MZ brightness from single sections of the brightest region of junctional Crb, corresponding to the MZ, using the line tool at 1 pixel width (narrower than the MZ). To measure apical Crb staining we used the brightest section just apical to the MZ and selected regular polygons just within the cell borders but excluding the cell periphery. We measured total Crb from maximal projections of five sections (0.3 µm apart) that encompassed the MZ, apical surface and underlying apical cytoplasm.

We measured both wt and *Moe* RNAi cells in each egg chamber, selecting the *z*-sections appropriate for wt and Moe-depleted cells (the apical of which was offset in the *z*-plane). For counts of Crb and Rab7 vesicles we

thresholded maximal projections of confocal *z*-series in ImageJ and used the Analyze Particles tool to count particles within manually outlined cells.

Acknowledgements
The authors thank Pam Vanderzalm, Adam Isabella and two anonymous reviewers for comments on the manuscript, and the Fehon, Rebay and Horne-Badovinac labs for helpful suggestions on this work. We also acknowledge numerous colleagues, the Developmental Studies Hybridoma Bank and the Bloomington *Drosophila* Stock Center [NIH P40OD018537] for providing antibodies and fly strains.

Competing interests
The authors declare no competing or financial interests.

Author contributions
K.M.S. and R.G.F. designed the experiments. K.M.S. performed the experiments, carried out data analysis and prepared figures. K.M.S. and R.G.F. wrote and edited the manuscript.

Funding
This work was funded by the National Institutes of Health [GM087588 to R.G.F.]. Deposited in PMC for release after 12 months.

Supplementary material
Supplementary material available online at
http://dev.biologists.org/lookup/suppl/doi:10.1242/dev.115329/-/DC1

References

Bazellieres, E. Assemat, E., Arsanto, J.-P., Le Bivic, A. and Massey-Harroche, D. (2009). Crumbs proteins in epithelial morphogenesis. *Front. Biosci.* **14**, 2149-2169.
Bretscher, A., Edwards, K. and Fehon, R. G. (2002). ERM proteins and merlin: integrators at the cell cortex. *Nat. Rev. Mol. Cell Biol.* **3**, 586-599.
Bulgakova, N. A. and Knust, E. (2009). The Crumbs complex: from epithelial-cell polarity to retinal degeneration. *J. Cell Sci.* **122**, 2587-2596.
Campbell, K., Knust, E. and Skaer, H. (2009). Crumbs stabilises epithelial polarity during tissue remodelling. *J. Cell Sci.* **122**, 2604-2612.
Cao, T. T., Deacon, H. W., Reczek, D., Bretscher, A. and von Zastrow, M. (1999). A kinase-regulated PDZ-domain interaction controls endocytic sorting of the beta2-adrenergic receptor. *Nature* **401**, 286-290.
D'Alterio, C., Tran, D. D. D., Au Yeung, M. W. Y., Hwang, M. S. H., Li, M. A., Arana, C. J., Mulligan, V. K., Kubesh, M., Sharma, P., Chase, M. et al. (2005). *Drosophila melanogaster* Cad99C, the orthologue of human Usher cadherin PCDH15, regulates the length of microvilli. *J. Cell Biol.* **171**, 549-558.
Delon, I. and Brown, N. H. (2009). The integrin adhesion complex changes its composition and function during morphogenesis of an epithelium. *J. Cell Sci.* **122**, 4363-4374.
Fehon, R. G., McClatchey, A. I. and Bretscher, A. (2010). Organizing the cell cortex: the role of ERM proteins. *Nat. Rev. Mol. Cell Biol.* **11**, 276-287.
Fletcher, G. C., Lucas, E. P., Brain, R., Tournier, A. and Thompson, B. J. (2012). Positive feedback and mutual antagonism combine to polarize crumbs in the Drosophila follicle cell epithelium. *Curr. Biol.* **22**, 1116-1122.
Goldenberg, G. and Harris, T. J. C. (2013). Adherens junction distribution mechanisms during cell-cell contact elongation in Drosophila. *PLoS ONE* **8**, e79613.
Gottlieb, T. A., Ivanov, I. E., Adesnik, M. and Sabatini, D. D. (1993). Actin microfilaments play a critical role in endocytosis at the apical but not the basolateral surface of polarized epithelial cells. *J. Cell Biol.* **120**, 695-710.
Grammont, M. (2007). Adherens junction remodeling by the Notch pathway in Drosophila melanogaster oogenesis. *J. Cell Biol.* **177**, 139-150.
Herranz, H., Stamataki, E., Feiguin, F. and Milán, M. (2006). Self-refinement of Notch activity through the transmembrane protein Crumbs: modulation of γ-secretase activity. *EMBO Rep.* **7**, 297-302.
Huang, J., Zhou, W., Dong, W., Watson, A. M. and Hong, Y. (2009). Directed, efficient, and versatile modifications of the *Drosophila* genome by genomic engineering. *Proc. Natl. Acad. Sci. USA* **106**, 8284-8289.
Izaddoost, S., Nam, S.-C., Bhat, M. A., Bellen, H. J. and Choi, K.-W. (2002). Drosophila Crumbs is a positional cue in photoreceptor adherens junctions and rhabdomeres. *Nature* **416**, 178-183.
Kaksonen, M., Toret, C. P. and Drubin, D. G. (2006). Harnessing actin dynamics for clathrin-mediated endocytosis. *Nat. Rev. Mol. Cell Biol.* **7**, 404-414.
Karagiosis, S. A. and Ready, D. F. (2004). Moesin contributes an essential structural role in Drosophila photoreceptor morphogenesis. *Development* **131**, 725-732.
Kempkens, Ö., Médina, E., Fernandez-Ballester, G., Özüyaman, S., Le Bivic, A., Serrano, L. and Knust, E. (2006). Computer modelling in combination with in vitro studies reveals similar binding affinities of Drosophila Crumbs for the PDZ domains of Stardust and DmPar-6. *Eur. J. Cell Biol.* **85**, 753-767.
Kerman, B. E., Cheshire, A. M., Myat, M. M. and Andrew, D. J. (2008). Ribbon modulates apical membrane during tube elongation through Crumbs and Moesin. *Dev. Biol.* **320**, 278-288.
Klebes, A. and Knust, E. (2000). A conserved motif in Crumbs is required for E-cadherin localisation and zonula adherens formation in Drosophila. *Curr. Biol.* **10**, 76-85.
Klose, S., Flores-Benitez, D., Riedel, F. and Knust, E. (2013). Fosmid-based structure-function analysis reveals functionally distinct domains in the cytoplasmic domain of Drosophila crumbs. *G3* **3**, 153-165.
Laprise, P., Beronja, S., Silva-Gagliardi, N. F., Pellikka, M., Jensen, A. M., McGlade, C. J. and Tepass, U. (2006). The FERM protein Yurt is a negative regulatory component of the Crumbs complex that controls epithelial polarity and apical membrane size. *Dev. Cell* **11**, 363-374.
Lecuit, T. and Pilot, F. (2003). Developmental control of cell morphogenesis: a focus on membrane growth. *Nat. Cell Biol.* **5**, 103-108.
Letizia, A., Sotillos, S., Campuzano, S. and Llimargas, M. (2011). Regulated Crb accumulation controls apical constriction and invagination in Drosophila tracheal cells. *J. Cell Sci.* **124**, 240-251.
Letizia, A., Ricardo, S., Moussian, B., Martin, N. and Llimargas, M. (2013). A functional role of the extracellular domain of Crumbs in cell architecture and apicobasal polarity. *J. Cell Sci.* **126**, 2157-2163.
Ling, C., Zheng, Y., Yin, F., Yu, J., Huang, J., Hong, Y., Wu, S. and Pan, D. (2010). The apical transmembrane protein Crumbs functions as a tumor suppressor that regulates Hippo signaling by binding to Expanded. *Proc. Natl. Acad. Sci. USA* **107**, 10532-10537.
Lu, H. and Bilder, D. (2005). Endocytic control of epithelial polarity and proliferation in *Drosophila*. *Nat. Cell Biol.* **7**, 1232-1239.
Matsui, T., Maeda, M., Doi, Y., Yonemura, S., Amano, M., Kaibuchi, K., Tsukita, S. and Tsukita, S. (1998). Rho-kinase phosphorylates COOH-terminal threonines of ezrin/radixin/moesin (ERM) proteins and regulates their head-to-tail association. *J. Cell Biol.* **140**, 647-657.
Médina, E., Williams, J., Klipfell, E., Zarnescu, D., Thomas, G. and Le Bivic, A. (2002a). Crumbs interacts with moesin and beta(Heavy)-spectrin in the apical membrane skeleton of Drosophila. *J. Cell Biol.* **158**, 941-951.
Médina, E., Lemmers, C., Lane-Guermonprez, L. and Le Bivic, A. (2002b). Role of the Crumbs complex in the regulation of junction formation in Drosophila and mammalian epithelial cells. *Biol. Cell.* **94**, 305-313.
Morais-de-Sá, E., Mirouse, V. and St Johnston, D. (2010). aPKC phosphorylation of Bazooka defines the apical/lateral border in Drosophila epithelial cells. *Cell* **141**, 509-523.
Muschalik, N. and Knust, E. (2011). Increased levels of the cytoplasmic domain of Crumbs repolarise developing Drosophila photoreceptors. *J. Cell Sci.* **124**, 3715-3725.
Neisch, A. L., Speck, O., Stronach, B. and Fehon, R. G. (2010). Rho1 regulates apoptosis via activation of the JNK signaling pathway at the plasma membrane. *J. Cell Biol.* **189**, 311-323.
Neisch, A. L., Formstecher, E. and Fehon, R. G. (2013). Conundrum, an ARHGAP18 orthologue, regulates RhoA and proliferation through interactions with Moesin. *Mol. Biol. Cell* **24**, 1420-1433.
Pellikka, M., Tanentzapf, G., Pinto, M., Smith, C., McGlade, C. J., Ready, D. F. and Tepass, U. (2002). Crumbs, the Drosophila homologue of human CRB1/RP12, is essential for photoreceptor morphogenesis. *Nature* **416**, 143-149.
Pilot, F., Philippe, J.-M., Lemmers, C. and Lecuit, T. (2006). Spatial control of actin organization at adherens junctions by a synaptotagmin-like protein. *Nature* **442**, 580-584.
Pocha, S. M. and Knust, E. (2013). Complexities of Crumbs function and regulation in tissue morphogenesis. *Curr. Biol.* **23**, R289-R293.
Pocha, S. M., Wassmer, T., Niehage, C., Hoflack, B. and Knust, E. (2011). Retromer controls epithelial cell polarity by trafficking the apical determinant Crumbs. *Curr. Biol.* **21**, 1111-1117.
Polesello, C., Delon, I., Valenti, P., Ferrer, P. and Payre, F. (2002). Dmoesin controls actin-based cell shape and polarity during Drosophila melanogaster oogenesis. *Nat. Cell Biol.* **4**, 782-789.
Pope, K. L. and Harris, T. J. C. (2008). Control of cell flattening and junctional remodeling during squamous epithelial morphogenesis in Drosophila. *Development* **135**, 2227-2238.
Richard, M., Muschalik, N., Grawe, F., Özüyaman, S. and Knust, E. (2009). A role for the extracellular domain of Crumbs in morphogenesis of Drosophila photoreceptor cells. *Eur. J. Cell Biol.* **88**, 765-777.
Robinson, B. S., Huang, J., Hong, Y. and Moberg, K. H. (2010). Crumbs regulates Salvador/Warts/Hippo signaling in Drosophila via the FERM-domain protein Expanded. *Curr. Biol.* **20**, 582-590.
Roh, M. H., Fan, S., Liu, C.-J. and Margolis, B. (2003). The Crumbs3-Pals1 complex participates in the establishment of polarity in mammalian epithelial cells. *J. Cell Sci.* **116**, 2895-2906.
Röper, K. (2012). Anisotropy of crumbs and aPKC drives myosin cable assembly during tube formation. *Dev. Cell* **23**, 939-953.
Schlichting, K., Wilsch-Bräuninger, M., Demontis, F. and Dahmann, C. (2006). Cadherin Cad99C is required for normal microvilli morphology in Drosophila follicle cells. *J. Cell Sci.* **119**, 1184-1195.

Development (2015) 142, 1869-1878 doi:10.1242/dev.115329

Schotman, H., Karhinen, L. and Rabouille, C. (2008). dGRASP-mediated noncanonical integrin secretion is required for Drosophila epithelial remodeling. *Dev. Cell* **14**, 171-182.

Speck, O., Hughes, S. C., Noren, N. K., Kulikauskas, R. M. and Fehon, R. G. (2003). Moesin functions antagonistically to the Rho pathway to maintain epithelial integrity. *Nature* **421**, 83-87.

Tanaka, T. and Nakamura, A. (2008). The endocytic pathway acts downstream of Oskar in Drosophila germ plasm assembly. *Development* **135**, 1107-1117.

Tanentzapf, G., Smith, C., McGlade, J. and Tepass, U. (2000). Apical, lateral, and basal polarization cues contribute to the development of the follicular epithelium during Drosophila oogenesis. *J. Cell Biol.* **151**, 891-904.

Tepass, U. (1996). Crumbs, a component of the apical membrane, is required for zonula adherens formation in primary epithelia of Drosophila. *Dev. Biol.* **177**, 217-225.

Tepass, U. (2012). The apical polarity protein network in Drosophila epithelial cells: regulation of polarity, junctions, morphogenesis, cell growth, and survival. *Ann. Rev. Cell. Dev. Biol.* **28**, 655-685.

Thompson, B. J., Pichaud, F. and Röper, K. (2013). Sticking together the Crumbs–an unexpected function for an old friend. *Nat. Rev. Mol. Cell Biol.* **14**, 307-314.

Wahlström, G., Norokorpi, H.-L. and Heino, T. I. (2006). Drosophila alpha-actinin in ovarian follicle cells is regulated by EGFR and Dpp signalling and required for cytoskeletal remodelling. *Mech. Dev.* **123**, 801-818.

Walther, R. F. and Pichaud, F. (2010). Crumbs/DaPKC-dependent apical exclusion of Bazooka promotes photoreceptor polarity remodeling. *Curr. Biol.* **20**, 1065-1074.

Whiteman, E. L., Fan, S., Harder, J. L., Walton, K. D., Liu, C.-J., Soofi, A., Fogg, V. C., Hershenson, M. B., Dressler, G. R., Deutsch, G. H. et al. (2013). Crumbs3 is essential for proper epithelial development and viability. *Mol. Cell. Biol.* **34**, 43-56.

Wodarz, A., Hinz, U., Engelbert, M. and Knust, E. (1995). Expression of crumbs confers apical character on plasma membrane domains of ectodermal epithelia of Drosophila. *Cell* **82**, 67-76.

Wu, X., Tanwar, P. S. and Raftery, L. A. (2008). Drosophila follicle cells: morphogenesis in an eggshell. *Semin. Cell Dev. Biol.* **19**, 271-282.

Zhou, B., Wu, Y. and Lin, X. (2011). Retromer regulates apical-basal polarity through recycling Crumbs. *Dev. Biol.* **360**, 87-95.

Supplementary Figures

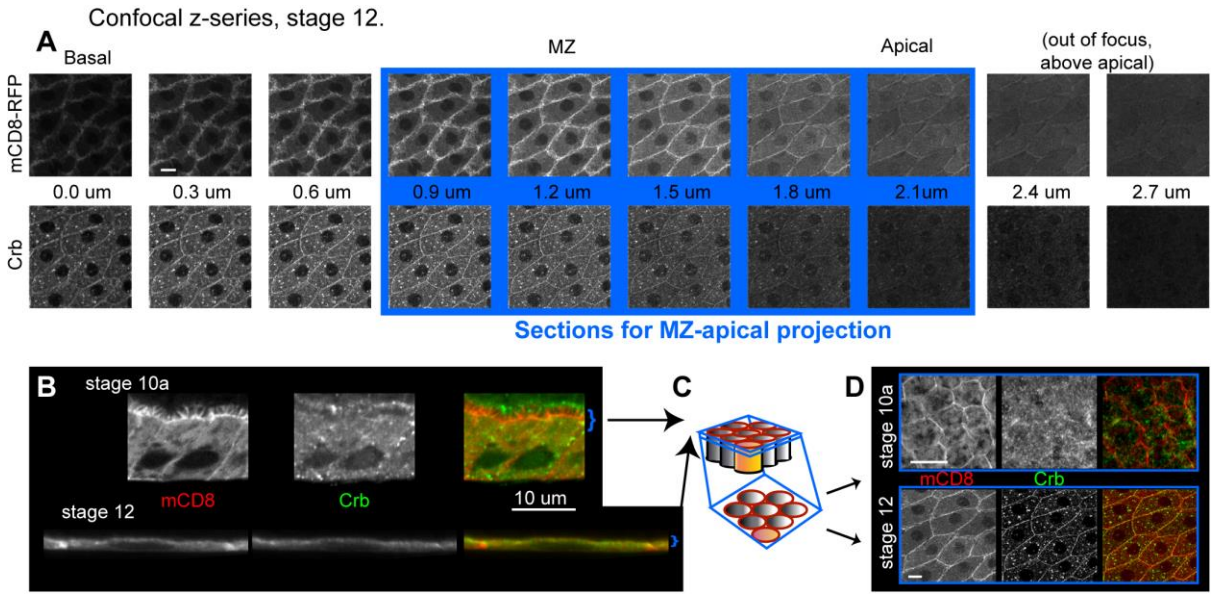

Figure S1. Method for distinguishing apical from junctional staining. (A) Representative z-series of ten 0.3- µm sections, stage 12 egg chamber co-stained with mCD8-RFP and Crb. (B) Cross-sectional images from a stage 10 and 12 egg chambers. (C) Cartoon showing projection of junctional-apical slices. (D) Resulting maximal projections of stage 10 and 12 MZ-apical region. See Materials and Methods for further detail. Scale bars: 10 µm.

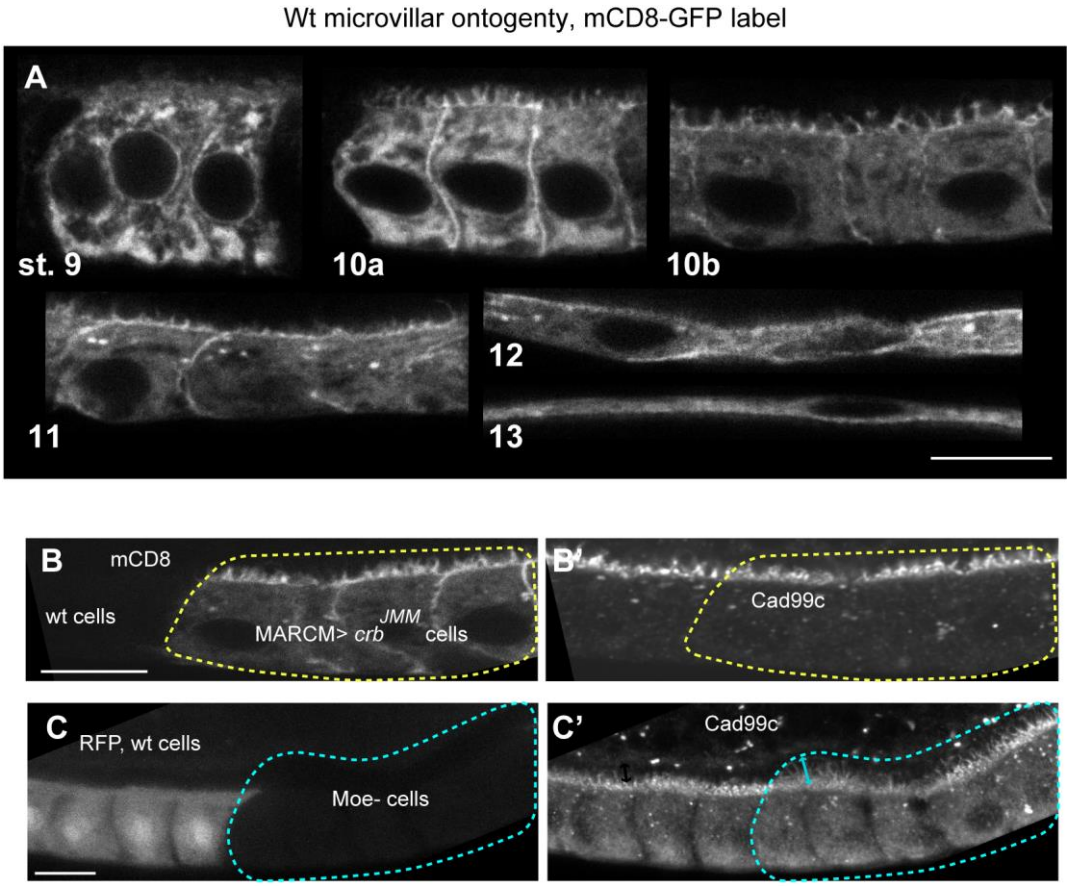

Figure S2. ***crb*** **and** ***Moe*** **phenotypes are not attributable to effects on microvilli.** (A) Normal MV ontogeny; outgrowth in stage 10a is followed by recession in stage 11. (B) Stage 10 crb^{JMM} clones had no microvillar phenotype. (C) Stage 10 *Moe*-null clones had abnormally long microvilli. Scale bars: 10 μm.

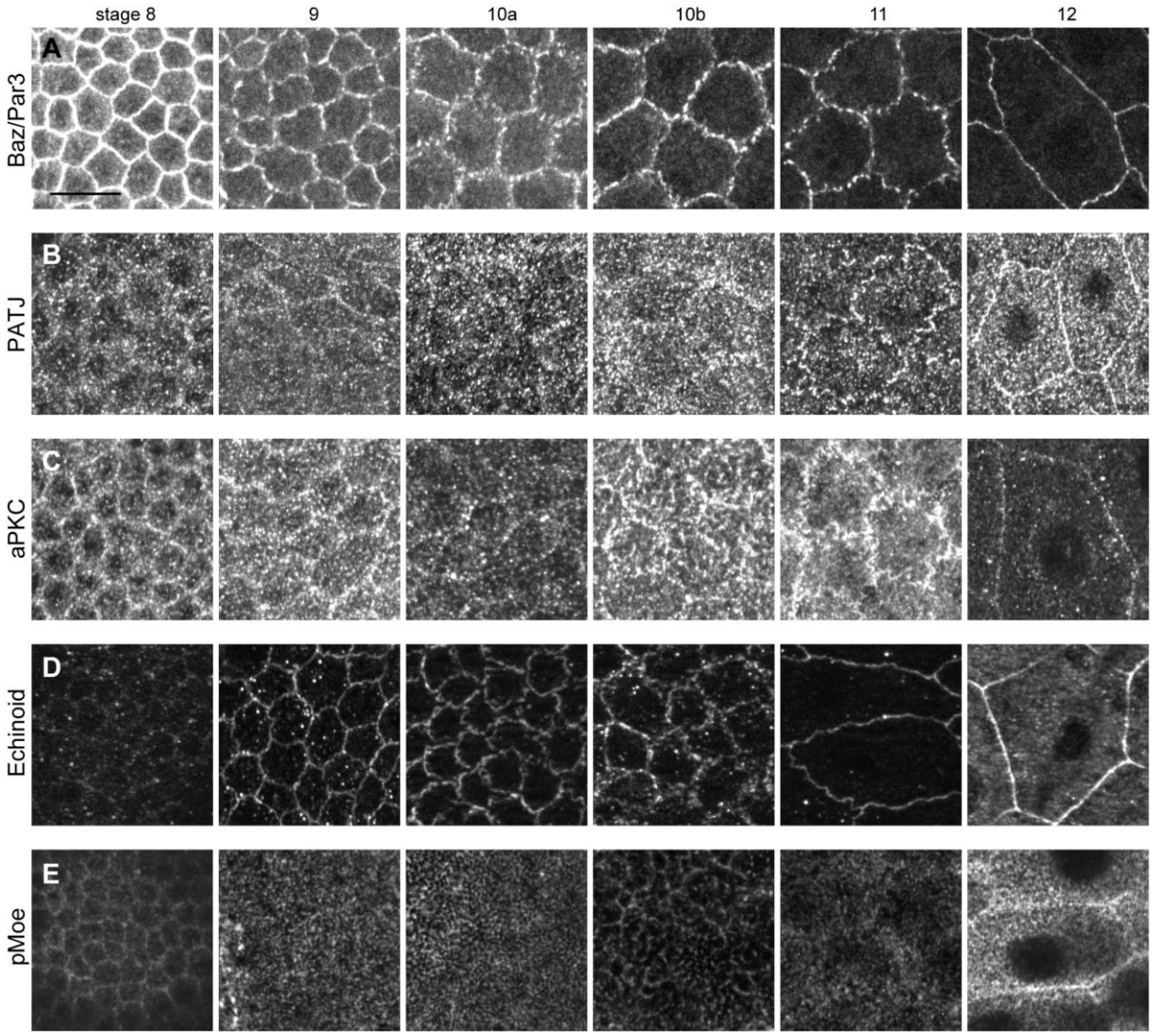

Figure S3. Ontogeny of apical-junctional stains in wild-type follicle cells. (A) Baz/Par3 displayed the same corrugations as Ecad in stages 9-10. These were also apparent in many of the MZ proteins in stage 11, including Patj (B) aPKC (C), and Echinoid (D), which, unlike Crb, remained at the MZ during stage 10, though sharpening in stage 11. pMoe, like Crb, was absent from the MZ in stage 9-10, returning in stage 11. Images of each stain taken with the same settings from the same slide, except Patj stage 8-9 9 and Echinoid stage 9. Scale bars: 10 μm.

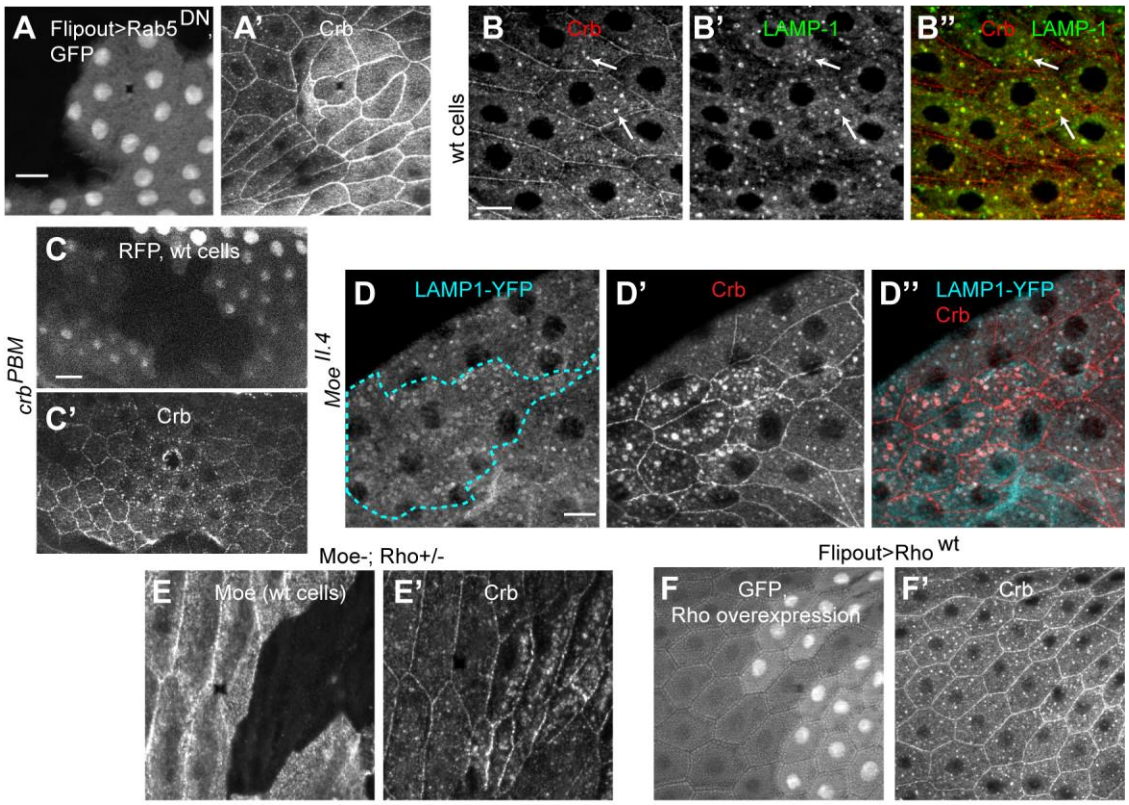

Figure S4. **Crb vesicles are endocytosed and degraded in stage 12 independently of Moe and of Rho.** (A) Crb vesicles were abrogated in Rab5^{DN}, stage 12. (B) Colocalization of Crb and the lysosomal marker Lamp-1 in wt follicle cells. (C) *crb*^{PBM} was excessively vesicular in stage 9. (D) The lysosomal marker Lamp-1 showed Crb was trafficked to the lysosome in Moe-depleted cells as in wt cells. (E,F) Moe-null effects on Crb are independent of Rho. (E) Rho depletion did not suppress Crb phenotype in Moe-null cells. (F) Rho overexpression did not phenocopy the Crb phenotype seen with Moe depletion. Images from stage 12 egg chambers, except C from stage 9. Scale bars: 10 µm.

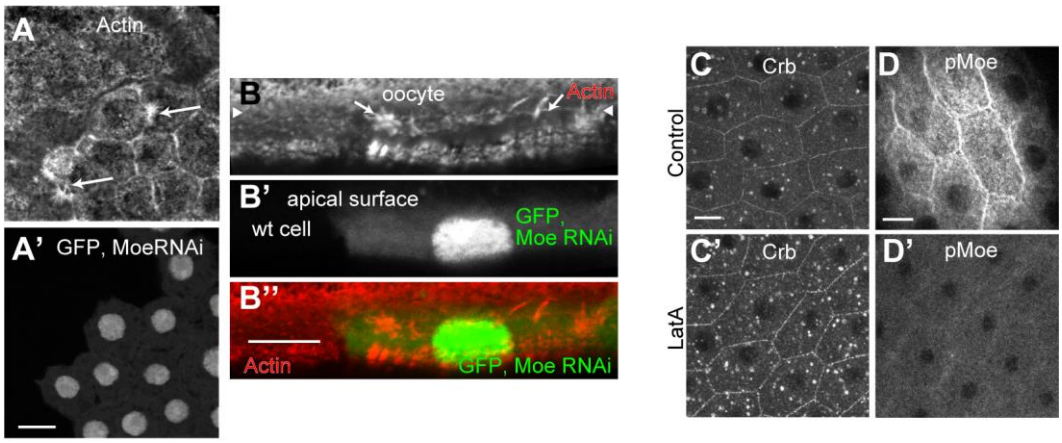

Figure S5. **Moe depletion causes actin defects associated with elevated Crb vesicles.** (A-B) Moe depletion caused aberrant actin structures (arrows) at the apical margins (A, apical section; B, cross-section; arrowheads in B mark apical surface of follicle cells). (C-C') Depolymerizing F-actin with latrunculin A caused buildup of MZ Crb and increase of vesicular Crb at stage 12, similar to Moe depletion; but also caused strong loss of pMoe (D-D'). All egg chambers stage 12. Scale bars: 10 µm.

Supplementary Table 1. Coimmunoprecipitation assays in *Drosophila* S2 cells of Crb with Moe or aPKC had negative results

IP bait	Co-IP targets
Flag-Moe$^{\Delta act}$	Myc-Crb^{i}, Myc-Crb$^{i\ JMM}$, Myc-Crb$^{i\ PBM}$
Flag-Moe^{T559D}	Myc-Crb^{i}, Myc-Crb$^{i\ JMM}$, Myc-Crb$^{i\ PBM}$
Flag-Crb^{i}	Myc-Moe$^{\Delta act}$, Myc-Moe^{T559D}, endogenous Moe, aPKC-GFP, endogenous aPKC
Flag-Crb$^{i\ JMM}$	Myc-Moe$^{\Delta act}$, Myc-Moe^{T559D}, endogenous Moe, aPKC-GFP, endogenous aPKC
Flag-Crb$^{i\ PBM}$	Myc-Moe$^{\Delta act}$, Myc-Moe^{T559D}, endogenous Moe, aPKC-GFP, endogenous aPKC
Flag-Crb$^{i\ T6AT9A}$	Myc-Moe$^{\Delta act}$, Myc-Moe^{T559D}, endogenous Moe, aPKC-GFP, endogenous aPKC
Flag-Crb$^{i\ T6DT9D}$	Myc-Moe$^{\Delta act}$, Myc-Moe^{T559D}, endogenous Moe, aPKC-GFP, endogenous aPKC
Myc-Moe$^{\Delta act}$	Flag-Crb^{i}, Flag-Crb$^{i\ JMM}$, Flag-Crb$^{i\ PBM}$, Flag-Crb$^{i\ T6AT9A}$, Flag-Crb$^{i\ T6DT9D}$
Myc-Moe^{T559D}	Flag-Crb^{i}, Flag-Crb$^{i\ JMM}$, Flag-Crb$^{i\ PBM}$, Flag-Crb$^{i\ T6AT9A}$, Flag-Crb$^{i\ T6DT9D}$
Myc-Crb^{i}	Flag-Moe$^{\Delta act}$, Flag-Moe^{T559D}, endogenous Moe, aPKC-GFP, endogenous aPKC
Myc-Crb$^{i\ JMM}$	Flag-Moe$^{\Delta act}$, Flag-Moe^{T559D}, endogenous Moe, aPKC-GFP, endogenous aPKC
Myc-Crb$^{i\ PBM}$	Flag-Moe$^{\Delta act}$, Flag-Moe^{T559D}, endogenous Moe, aPKC-GFP, endogenous aPKC

In all cases, target proteins were detected in lysates and IPs were strong, but in no case was a Co-IP seen above levels of negative controls. Flag IPs were performed as in Neisch et al. (2010), using Sigma Flag beads; Myc IPs were performed by labeling protein G beads with mouse anti-Myc for 2-12 hours. Myc-Crb^{i} constructs gift of D. Pan; Flag-Crb^{i} constructs created by C. Horth, based on Myc-Crb^{i}.